Temporal Changes in Quasar Broad Emission Line Profiles and the Gravitationally Lensed Nature of Q1634+267A,B and Q2345+007A,B

Todd A. Small[1], Wallace L.W. Sargent, and Charles C. Steidel
Palomar Observatory, California Institute of Technology, Pasadena, CA 91125
Electronic mail: tas@ast.cam.ac.uk; wws,ccs@astro.caltech.edu

ABSTRACT

Steidel & Sargent (1991a) found that the spectra of the components of the close quasar pairs Q1634+267A,B and Q2345+007A,B were in each case remarkably similar (except for overall differences in brightness) but that individual broad emission lines due to Ly α, Si IV, C IV and C III] exhibited differences in profile or equivalent width between the A and B components. If the A and B components of these objects result from gravitational lensing of a single QSO, the difference in light travel time for the two images is roughly one year for both pairs. Accordingly, the authors suggested that observations of the spectra of single QSOs would reveal similar changes in emission line profiles and equivalent widths on a time scale of one year or less. In order to test Steidel & Sargent's (1991a) hypothesis, we obtained in 1992 high quality spectra of 30 quasars with $z_{em} \sim 1$ selected from the brighter QSOs in the sample of Steidel & Sargent (1991b), which those authors had observed in 1989–90. The new spectra were obtained with exactly the same instrumental setup as the earlier observations. The two sets of spectra were reduced in an identical manner and then compared in order to search for changes in the strengths and profiles of the principal emission lines occurring on time scales of order one year. We find that the spectra from the two epochs are remarkably similar for all the QS0s, except for overall changes in fluxes and minor differences in continuum shape which are probably artifacts introduced by the observing procedures. However, there are also changes in the equivalent widths or shapes of the stronger emission lines on rest-frame time scales of 1-1.5 years in about two thirds of the QSOs. These observations, therefore, support the notion that Q1634+267A,B and Q2345+007A,B are gravitationally lensed and that the spectra of the components in lensed QSOs need not be exactly identical. Moreover, it should be expected that any differences between the components in such systems should change with time.

[1]present address: Institute of Astronomy, University of Cambridge, Madingley Road, Cambridge CB3 0HA, United Kingdom

1. Introduction

The nature of two close pairs of QSOs, Q1634+267A,B (separation 3.77″) and Q2345+007A,B (7.03″) is still not established with certainty. In both cases, the two components of the pair have the same redshift within the errors of measurement and, as a result, they have both been considered likely to result from gravitational lensing of a single QSO (Djorgovski & Spinrad 1994, Weedman et al. 1982). However, a candidate for the lens has not been established with certainty in either case, despite the fact that such wide spacings require either an unusually massive galaxy or a cluster of galaxies. Deep infrared observations at the Keck 10-meter telescope of Q1634+267A,B have not revealed a candidate lensing galaxy down to a 3.5 σ detection limit of K = 21.3 mag, although we note as well that the object responsible for the strong absorption line system at $z \approx 1.126$ was also not detected (Neugebauer et al. 1993, J. Larkin, personal communication). A $B_{\rm J} = 25.0$ lens candidate for Q2345+007A,B has recently been detected by Fischer et al. (1994) northeast of image B, but it will take at least a 10-meter-class telescope to measure the redshift of the candidate. Bonnet et al. (1993) have both reported arclets and lensing-induced distortions of faint galaxies near the pair, which is further evidence for the presence of a massive lens. Using redshifts of galaxies in the field of Q2345+007A,B estimated with multi-color photometry, Pelló et al. (1996) have found evidence for a cluster of galaxies at $z \approx 0.78$, but the cluster core lies 45″ away from the lensed pair. Accordingly, the possibility is still entertained that the pairs are binary QSOs with separations of a few tens of kpc. A resolution of the question is of considerable importance because such QSO pairs are essential for measuring the sizes of the intervening absorption systems (see, e.g., Foltz et al. 1984; Duncan 1991; McGill 1991; Steidel & Sargent 1991a; Bechtold et al. 1994; Dinshaw et al. 1994, 1995); however, the limits determined for the sizes depend strongly on whether a particular close pair is a manifestation of lensing or a real binary QSO.

Steidel & Sargent (1991a) recorded high signal-to-noise ratio spectra of the QSO pairs Q1634+267A,B and Q2345+007A,B in order to examine critically the degree of similarity of the two components in each pair. The two components were observed *simultaneously* with a long slit. They found that the overall continuum shapes in the spectra of each pair were remarkably similar and that, in general, the emission lines closely matched. However, they also discovered that the Ly α, N V, C IV, and Si IV emission lines of the two images of Q1634+267A,B exhibit differences in profile, which they described as velocity shifts of as much as $\sim$ 1000 km s^{-1}. On the other hand, while the redshifts of the emission lines in the spectra of Q2345+007A,B are indistinguishable within the measurement errors, ($\Delta v_{B-A} = 15 \pm 20$ km s^{-1}), the Ly α and, particularly, the C III] emission lines differ significantly in strength in the two spectra. Because of the remarkable overall similarity of the spectra of the components within each pair, Steidel & Sargent (1991a) concluded that both Q1634+267A,B and Q2345+007A,B result from gravitational lensing. Since the prominent spectral differences are too large to be comfortably accommodated as microlensing by stars in the lens (Nemiroff 1988, Schneider & Wambsganss 1990), they ascribed the differences to intrinsic emission line profile variations on a characteristic time scale less than the time delays

between the light travel times of the two images, which are roughly one year for both pairs.

Variability in the strengths and profiles of quasar broad emission lines on year and shorter time scales has been reported by a number of workers (e.g., Zheng et al. 1987; O'Brien, Zheng, & Wilson 1989; and Gondhalekar 1990), but these reports have been based on either observations of the Balmer lines or on comparatively noisy spectra of the high-ionization ultraviolet lines obtained with *International Ultraviolet Explorer* satellite. Following Steidel & Sargent's (1991a) work, Corbin (1992) announced that he had discovered increases in the equivalent widths acccompanied by shifts of 2200 km s^{-1} in the redshifts of the C III] emission line in the spectra of two QSOs. The spectra had been observed 1.5 years apart. This work has not been fully published or critically assessed and, even if it proves to be correct, there is no information on the ubiquity of such behavior, although there have been other reports of profile differences in the broad lines of candidate gravitationally-lensed quasars pairs (e.g., Filippenko 1989, Wisotzki et al. 1995, Impey et al. 1996). In particular, there are two reports of dramatic velocity differences similar to those described by Steidel & Sargent (1991a) . Saunders et al. (1997) argue that the quasar pair PC 1643+4631A,B ($z = 3.79, 3.83$, separation $198''$) is lensed by a cluster responsible for the cosmic microwave background decrement detected by Jones et al. (1997) in the direction of the quasar pair. Michalitsianos et al. (1997) describe a velocity difference of $\sim 600 - 700$ km s^{-1} between the broad emission lines of UM425A,B, a pair of $z \approx 1.47$ quasars with a $6.5''$ separation.

There is a persuasive indirect argument for believing that the centroid velocities of the broad emission lines in QSOs must vary. Namely, it is observed that the velocities determined from different ions in a quasar spectrum often differ by ~ 1000 km s^{-1}. Since the distribution of velocity differences is broad with a mode that is consistent with 0 km s^{-1} (Steidel & Sargent 1991b), it is likely that these velocity differences reflect variability in the velocities of the broad lines, although on an unknown time scale.

Based on the above considerations, we decided to search for emission line profile and velocity changes in single QSOs by reobserving 30 objects from the Mg II survey of Steidel & Sargent (1992) , using an identical instrument configuration. The spectra used in the survey were obtained for measuring *absorption* lines, in particular, the Mg II $\lambda\lambda$2796,2803 doublet; accordingly, their S/N ratio is exceptionally high. In order to study the cosmological evolution of Mg II absorption, the QSOs were selected to have redshifts in two ranges, one around $z_{em} \sim 1.2$ and the other around $z_{em} \sim 2$. In general, the spectra cover the wavelength region from below the C III] λ1909 emission line to above the Mg II λ2800 emission line. We chose to repeat only spectra of QSOs in the lower redshift range because the sky subtraction is much harder for QSOs in the higher redshift range. We also elected to reobserve the brighter QSOs in the original survey where possible. The observing and data reduction procedures are described in § 2, an analysis of the spectral differences between the two epochs is given in § 3, and we discuss our conclusions in § 4.

2. Observations and Data Reduction

We have reobserved 30 quasars with $z \sim 1$ from the survey of Steidel & Sargent (1992). We used an identical instrumental setup: the Double Spectrograph attached to the 5.08m Hale Telescope, covering the spectral range from 3100 - 7000Å with $\sim$ 4Å resolution for wavelengths $\lesssim$ 4700 Å (the blue side) and $\sim$ 6Å resolution for wavelengths $\gtrsim$ 4700 Å (the red side). The observations were made with a $1''$ slit. A journal of our observations is presented in Table 1. We were careful to set the position angle of the slit to the parallactic angle appropriate to the midpoint of the observation in order to minimize light losses at the blue end of the spectrum. However, because of seeing fluctuations and the narrow entrance slit, we can say nothing about changes in continuum fluxes. Moreover, the possibility of guiding errors, together with the fact that the position angle of the slit was not adjusted during the typically hour-long exposures, means that apparent changes in the overall continuum slopes between the two epochs cannot be trusted.

Our data were reduced using standard techniques and routines from IRAF. The spectra were flux-calibrated using instrumental sensitivity functions determined from observations of spectrophotometric standards. The spectra usually matched at the overlap region between the blue and red cameras. We found that while our reductions of the original data of Steidel & Sargent (1992) agreed very well in the red, there was significant disagreement in the blue. This disagreement is due to the fact that Steidel & Sargent (1992) used the airmass at the end of the exposure[2], which is the airmass recorded in the image headers at Palomar, to compute the extinction correction; whereas, we used the mean airmass appropriate for the whole exposure. The comparisons between the two epochs are based exclusively on the re-reduced data.

3. Analysis

3.1. Comparison of the Spectra

As described above (§ 2), we do not trust apparent changes in the continua between the two epochs, primarily because of our use of a narrow slit. Since in this study we are only interested in the emission lines, we have chosen to remove the continuum variations by fitting 5 piece cubic splines to the spectra. The composite QSO spectrum synthesized by Francis et al. (1991) from 718 individual spectra has many emission lines with few gaps where continuum may be present. Accordingly, our fits are not meant to be accurate representations of the true quasar continua. The fits were arranged to ignore the broad emission lines and the narrow absorption lines by using a rejection threshold of 2 σ for positive deviations and a threshold of 4 σ for negative deviations. As can be seen in Figure 1, the continuum-flattened spectra from the two epochs match very well.

[2]Since Steidel & Sargent (1992) were searching for absorption lines, the errors caused by using the airmass at the end of the exposure have no effect on their analysis.

However, there is a distinct tendency for the blue sections of the spectra to agree better than the red sections. This is surprising because both guiding errors and the incomplete correction for atmospheric dispersion would be expected to have a greater effect on the repeatabilty of the blue ends of the spectra. However, the red camera of the Double Spectrograph was prone to ice on the dewar window which was hard to recognize during the course of observations until the effects become very severe.

3.2. Notes on Individual Objects

We have compared the spectra of each QSO obtained at the two epochs in two ways. First we compared the blue and red spectra shown in Figure 1 separately, then we compared the complete spectra. For this latter purpose color renditions of the spectra obtained at the two epochs were superimposed; these color pictures are not reproduced here, but digital copies can be supplied to interested readers on request to the first author. Our conclusions regarding changes in the spectra of each object are given below.

a) Q0024+2225; $z_{em} = 1.118$. The continuum-normalized spectra match very well except below 3200 Å. The prominent broad emission lines, C IV, C III], and Mg II, are all stronger in the first epoch spectrum.

b) Q0117+2118; $z_{em} = 1.493$. The spectra from the two epochs are in excellent agreement except for the Si IV line, which is stronger in the first epoch spectrum.

c) Q0232-0415; $z_{em} = 1.434$. While the red side spectra agree satisfactorily, the blue side spectra agree quite poorly. Both C IV and C III] exhibit dramatic changes in equivalent width. We believe that the the change in C IV is real; the apparent change in C III] could arise from problems with the calibration of the spectra near the dichroic changeover. The pair of emission lines at ~ 4000 Å, He II $\lambda1640$ and O III] $\lambda1663$, appear to be resolved in the second epoch spectrum and merged together at the first epoch. An examination of the other spectra in our sample reveals that the resolution of these features varies considerably from object to object.

d) Q0248+4302; $z_{em} = 1.316$. The spectra match astonishingly well. Spectra like these help give credence to the reality of the apparent changes in other spectra in the sample. The broad emissions lines are all stronger in the first epoch spectrum.

e) Q0333+3208; $z_{em} = 1.263$. Both C III] and Mg II appear stronger in the second epoch spectra.

f) Q0454+0356; $z_{em} = 1.345$. The spectra from the two epochs match very well, and there is notably good agreement between the many absorption lines. The broad emission lines, particularly C III], are stronger in the first epoch spectrum. In addition, C IV shows slight but significant profile differences.

g) Q0856+4649; $z_{em} = 0.924$. There are no believable changes.

h) Q0859-1403; $z_{em} = 1.327$. The spectra from the two epochs match well. The C IV and C III] lines were stronger in the first epoch spectrum.

i) Q0946+3009; $z_{em} = 1.216$. This is a BAL QSO. The C IV and Mg II emission lines were stronger in the first epoch spectrum. The red continua match particularly well.

j) Q1019+3056; $z_{em} = 1.316$. The spectra from the two epochs agree very well except that the broad emission lines are somewhat stronger in the first epoch spectrum.

k) Q1038+0625; $z_{em} = 1.270$. The spectra from the two epochs match well.

l) Q1120+0154; $z_{em} = 1.490$. The spectra from the two epochs match nicely; however, the complex BAL absorption blueward of C IV appears to have changed. We judge the apparent changes in C III] and Mg II to be uncertain because the lines fall in the dichroic crossover region and the extreme red end of the spectra, respectively. Neither Si IV nor C IV show anys signs of variation.

m) Q1206+4557; $z_{em} = 1.158$. The spectra agree nicely; however, the C IV, C III] and Mg II emission lines are all slightly stronger in the second epoch spectrum.

n) Q1241+1737; $z_{em} = 1.273$. The spectra match well everywhere.

o) Q1254+0443; $z_{em} = 1.024$. Mg II in the second epoch spectrum is marginally stronger; otherwise, the spectra agree well. The C III], Al III complex has an unusual profile at both epochs.

p) Q1317+2743; $z_{em} = 1.022$. The spectra measured at the two epochs match satisfactorily. An unidentified feature observed at ≈ 4200 Å is stronger in the first epoch spectrum, as are the red wing and center of the Mg II emission line.

q) Q1338+4138; $z_{em} = 1.219$ Apart from poor agreement and excessive noise around the dichroic changeover, the spectra from the two epochs match well. The Mg II and C IV emission lines show no changes, but the red wing of the C III] line is higher at the earlier epoch, as is an unidentified feature at ≈ 5150 Å. The variation of the C III] profile is reminiscent of the variation in N V observed by Steidel & Sargent (1991a) in Q1634+267A,B.

r) Q1340+2859; $z_{em} = 0.905$. The spectra from the two epochs agree satisfactorily as does the Mg II profile. However, C III] is wider in the second epoch spectrum. A sharp [Ne V] $\lambda 3425$ emission line is exactly the same at each epoch.

s) Q1356+5806; $z_{em} = 1.371$. The spectra match well. The equivalent widths of the C IV, C III] and Mg II emission lines are greater in the first epoch spectrum.

t) Q1407+2632; $z_{em} = 0.944$. The complex spectra match very well. The emission lines look very unusual; the Fe II lines are very strong, and C III] and Mg II are remarkably weak.

u) Q1458+7152; $z_{em} = 0.905$. The emission lines are unusually sharp; C III] and Mg II are substantially stronger in the second epoch spectrum. The [Ne V] $\lambda3425$ emission line is stronger in the second epoch spectrum as well.

v) Q1522+1009; $z_{em} = 1.321$. The first epoch spectrum was recorded with the red camera grating inadvertently adjusted to give a central wavelength $\sim$ 200 Å to the red, and thus the continuum of the spectrum near the dichroic changeover is quite uncertain. Otherwise, the spectra agree well. Mg II is stronger and wider at the first epoch. With less certainty C IV is stronger at the second epoch.

w) Q1538+4745; $z_{em} = 0.770$. The spectra and the Mg II emission line profiles agree very well. A sharp [O II] $\lambda3727$ emission line is visible at both epochs. The C III] emission line is conspicuously wider in the first epoch spectrum, due to a stronger blue wing.

x) Q1634+7037; $z_{em} = 1.334$. The blue halves match very well. Unfortunately, Steidel & Sargent did not take a usable standard star for the red camera on the night that this object was observed during the first epoch, and so the best we can do for flux calibration is to use a red camera sensitivity function from another night. There is poor agreement near the dichroic changeover. In view of the flaws in the data, it is difficult to believe in the reality of the differences in the red spectra. There is marginal evidence that C III] is stronger in the first epoch spectrum.

y) Q1637+5726; $z_{em} = 0.745$. The spectra match unusually poorly, especially in the blue spectra. Mg II is noticeably stronger in the first epoch spectra. C III] appears to be stronger, too, but the increased noise in the far blue end of the spectrum makes this assessment less reliable. The narrow forbidden lines redward of Mg II, especially [O II], agree nicely.

z) Q1656+0519; $z_{em} = 0.887$. These complex spectra match well.

aa) Q1718+4806; $z_{em} = 1.084$. The spectra from the two epochs agree comparatively poorly. The broad emission lines agree well, however.

bb) Q1821+1042; $z_{em} = 1.360$. The spectra from the two epochs agree well. The C IV line is identical, while C III] and Mg II are slightly wider and stronger at the first epoch.

cc) Q2145+0643; $z_{em} = 0.990$. The spectra from the two epochs agree well except near the dichroic changeover. Mg II is slightly stronger in the first epoch spectrum. For another project, we obtained an additional spectrum of this quasar on 1992 October 20 ($\sim$ 4 months after the second epoch spectrum) with the same instrument configuration. In Figure 2, we plot the second epoch spectrum and the 1992 October 20 spectrum. Despite the short time interval between the two observations, we find significant changes in the strengths of C III] and Mg II.

dd) Q2216-0350; $z_{em} = 0.901$. The red side matches well; the blue side merely satisfactorily. Mg II is stronger at the second epoch. A weak, sharp [Ne V] $\lambda3425$ emission line is identical in the two spectra.

3.3. Cross-correlation analysis

Close visual inspection of the spectra reveals no significant emission line velocity shifts; however, we have also performed a cross-correlation analysis of the spectra to search systematically for such shifts. The results are summarized in Table 2 and in Figure 3. We cross-correlated three emission lines, C IV, C III], and Mg II, choosing sample regions corresponding to the extent of the emission lines measured by Francis et al. (1991) in their composite quasar spectrum. The cross-correlation results are not terribly sensitive to the precise wavelength interval chosen; increasing the windows by up to 50Å on both ends changes the measured velocity differences by only $\approx$ 80 km s^{-1}. The results are consistent with our impressions from a visual examination of spectra, namely that there are no significant shifts. Although the formal errors from the cross-correlation analysis (based on the formulae given in Tonry & Davis [1979]), are often only 10 or 20 km s^{-1}, we took the true error to be the rms velocity difference of the quasar pairs when the whole wavelength range from 3000 Å to 7000 Å was correlated. This value is 100 km s^{-1}. (In cases in which the formal error is actually larger than 100 km s^{-1}, we have simply used the formal error.) Using this estimate of the error, the cross-correlation analysis finds four apparently significant shifts between the two epochs, Q0454+0356 C IV, Q1120+0154 C III], Q1407+2632 C III], and Q1538+4745 C III]. The velocity differences found for Q0454+0356 C IV and Q1538+4745 C III] agree with our visual impressions. The results for Q1120+0154 C III] and Q1407+2632 C III] are not likely to be reliable because, in the first case, the line lies on the dichroic changeover and, in the second case, the line is unusually weak and broad. Moreover, based on our detailed examination of the spectra, we believe that a simple velocity shift obtained from a cross-correlation analysis gives a poor description of the complex emission line profile changes actually observed. Nevertheless, we note that we have computed the velocity shifts of Lyα and C IV in Steidel & Sargent's (1991a) original spectra of Q1634+267 by cross-correlating the spectra of A and B and have found that the shifts are $\sim$300-500 km s^{-1}, not $\sim$1000 km s^{-1} as these authors reported.

4. Discussion

Many of the QSOs in our sample exhibit temporal variations in the profiles of the broad emission lines similar to the observed differences in line profile between the A and B images of Q1623+267 and Q2345+007. These variations occur on time scales of 1-1.5 years in the rest frames of the QSOs. Accordingly, the relatively subtle differences in the broad emission line profiles in these close pairs could be due to the roughly one year difference in light travel time between the A and B components. Consequently, our study supports Steidel & Sargent's (1991a) conclusion that Q1634+267A,B and Q2345+007A,B are lensed quasars and not physical binary quasars. In addition, our study highlights the fact that the spectra of the components of a lensed quasar need not be identical and that the differences should be expected to change with time.

In order to establish beyond doubt that Q1634+267A,B and Q2345+007A,B are lensed systems, we suggest searching for correlated amplification changes in the system on time scales of a year and making high sensitivity radio observations of the system, similar to the one that Djorgovski et al. (1987) used to prove that Q1145-071A,B was *not* a lensed system. We note that Patnaik, Schneider, & Narayan (1996) have found weak radio emission from Q1634+267A and the limit on the emission from the B component is consistent with the optical brightness ratio. The approach of Bonnet et al. (1993) and Pelló et al. (1996) of using weak gravitational lensing to identify mass concentrations in the field Q2345+007A,B also appears to be promising, but the possible massive cluster inferred from their data requires spectroscopic confirmation.

We are grateful to the staff of the Palomar Observatory for making these observations possible. The comments of the referee, Craig Foltz, helped us to improve the presentation. This work has been supported in part by NSF Grant No. AST-92213165 (W.S.), an NSF Graduate Fellowship (T.S.), and by NASA through Grant No. HF-1008.01-90A awarded by the Space Telescope Science Institute which is operated by the AURA, Inc. for NASA under Contract No. NAS5-26555 (C.S.).

REFERENCES

Bechtold, J., Crotts, A., Duncan, R., & Fang, Y. 1994, ApJ, 437, L83

Bonnet, H., Fort, B., Kneib J.-P., Mellier, Y. & Soucail, G. 1993, A&A, 280, L7

Corbin, M.R. 1992, BAAS, 24, 744

Dinshaw, N., Impey, C., Foltz, C., Weymann, R., & Chaffee, F. 1994, ApJ, L87

Dinshaw, N., Foltz, C., Impey, C., Weymann, R., & Morris, S. 1995, Nature, 373, 223

Djorgovski, S., & Spinrad, H. 1984, ApJ, 282, L1

Djorgovski, S., Perley, R., Meylan, G., & McCarthy, P. 1987, ApJ, 321, L17

Duncan, R.C. 1991, ApJ, 375, L41

Filippenko, A. 1989, ApJ, 338, L49

Fischer, P., Tyson, J., Bernstein, G. & Guhathakurta, P. 1994, ApJ, 431, L71

Foltz, C.B., Weymann, R.J., Roser, H.J., & Chaffee, F.H. 1984, ApJ, 281, L1

Francis, P., Hewett, P., Foltz, C., Chaffee, F., Weymann, R., & Morris, S. 1991, ApJ, 373, 464

Gondhalekar, P. 1990, MNRAS, 243, 443

Jones, M., et al. 1997, ApJ, 479, L1

Impey, C., Foltz, C., Petry, C., Browne, I., & Patnaik, A. 1996, ApJ, 462, L53

Michalitsianos, A., Falco, E., Muñoz, J., Hintzen, P., & Kazanas, D. 1997, preprint (astro-ph/9707254)

McGill, C. 1991, MNRAS, 242, 544

Nemiroff, R. 1988, ApJ, 335, 593

Neugebauer, G. et al. 1993, BAAS, 25, 927

O'Brien, P., Zheng, W., & Wilson, R. 1989, MNRAS, 240, 741

Patnaik, A., Schneider, P., & Narayan, R. 1996, MNRAS, 281, L17

Pelló, R., Miralles, J., Leborgue, J.-F., Picat, J.-P., Soucail, G., & Bruzual, G. 1996, A&A, 314, 73

Saunders, R., et al. 1997, ApJ, 479, L5

Schneider, P., & Wambsganss, J. 1990, A&A, 237, 42

Steidel, C., & Sargent, W. 1991a, AJ, 102, 1610

Steidel, C., & Sargent, W. 1991b, ApJ, 382, 433

Steidel, C., & Sargent, W. 1992, ApJS, 80, 1

Tonry, J., & Davis, M. 1979, AJ, 84, 1511

Weedman, D., Weymann, R., Green, R., & Heckman, T. 1982, ApJ, 255, L5

Wisotzki, L., Köhler, T., Ikonomou, M., & Reimers, D. 1995, å, 297, L59

Zheng, W., Burbidge, E., Smith, H., Cohen, R., & Bradley, S. 1987, ApJ, 322, 164

Table 1. Journal of Observations

Quasar	z_{em}	Date (UT) 1[st] Epoch	2[nd] Epoch	Type[a]
Q0024+2225	1.118	1989 Jul 13	1992 Jan 31	R
Q0117+2118	1.493	1989 Nov 25	1992 Jan 31	U
Q0232−0415	1.434	1989 Nov 25	1992 Jan 31	R
Q0248+4302	1.316	1989 Nov 25	1992 Jan 31	R
		1989 Nov 27		
		1990 Jan 20		
Q0333+3208	1.263	1989 Nov 25	1992 Jan 31	R
		1990 Jan 21		
Q0454+0356	1.345	1989 Nov 25	1992 Jan 31	R
		1990 Jan 20		
Q0856+4649	0.924	1990 Jan 22	1992 Jan 30	U
Q0859−1403	1.327	1990 Jan 22	1992 Jan 31	Rs
Q0946+3009	1.216	1990 Jan 21	1992 Jan 30	U
Q1019+3056	1.316	1990 Jan 22	1992 Jan 31	Rs
Q1038+0625	1.270	1990 Jan 21	1992 Jan 31	Rs
Q1120+0154	1.490	1990 Jan 22	1992 Jan 30	S
Q1206+4557	1.158	1989 Jul 14	1992 Jan 31	U
Q1241+1737	1.273	1989 Jul 13	1992 Jan 31	U
Q1254+0443	1.024	1990 Jan 20	1992 Jan 31	U
Q1317+2743	1.022	1989 Jul 12	1992 Jan 31	R
Q1338+4138	1.219	1989 Jul 13	1992 Jan 31	U
Q1340+2859	0.905	1989 Jul 14	1992 Jun 26	R
Q1356+5806	1.371	1989 Jul 13	1992 Jun 26	R
Q1407+2632	0.944	1989 Jul 13	1992 Jan 30	Rs
Q1458+7152	0.905	1989 Jul 12	1992 Jun 26	Rs
Q1522+1009	1.321	1989 Jul 11	1992 Jun 26	U
Q1538+4745	0.770	1989 Jul 14	1992 Jun 26	U
Q1634+7037	1.334	1989 Jul 11	1992 Jun 25	U
Q1637+5726	0.745	1989 Jul 13	1992 Jun 26	R
Q1656+0519	0.887	1989 Jul 11	1992 Jun 25	R
Q1718+4807	1.084	1989 Jul 11	1992 Jun 25	U
Q1821+1042	1.360	1989 Jul 11	1992 Jun 25	R
Q2145+0643	0.990	1989 Jul 11	1992 Jun 26	R
Q2216−0350	0.901	1989 Jul 14	1992 Jun 26	R

[a]Method of original discovery: “R” denotes radio selected, where “Rs” denotes “steep” radio spectrum ($\alpha > 0.5$, $f_\nu \propto \nu^{-\alpha}$), “U” denotes ultraviolet excess, and “S” denotes slitless spectroscopy.

TABLE 2

CROSS-CORRELATION RESULTS

Quasar	Whole Spectrum		C IV λ1549		C III] λ1909		Mg II λ2800	
	Δv (km s^{-1})[a]	CCF[b]	Δv (km s^{-1})	CCF	Δv (km s^{-1})	CCF	Δv (km s^{-1})	CCF
Q0024+2225	6 ±107	0.91	···	···	-36 ±3	0.97	-53 ±40	0.97
Q0117+2118	-60 ±34	0.94	-76 ±12	0.97	-18 ±27	0.96	···	···
Q0232−0415	15 ±170	0.91	71 ±28	0.96	-137 ±149	0.92	···	···
Q0248+4302	-27 ±62	0.83	1 ±20	0.97	-78 ±55	0.93	-47 ±25	0.99
Q0333+3208	-20 ±63	0.85	123 ±66	0.89	-271 ±24	0.94	-134 ±57	0.95
Q0454+0356	-75 ±36	0.94	-354 ±45	0.98	-133 ±16	0.95	···	···
Q0856+4649	-62 ±57	0.94	···	···	-144 ±27	0.99	-104 ±24	0.99
Q0859−1403	92 ±129	0.93	117 ±64	0.98	-24 ±23	0.98	···	···
Q0946+3009	52 ±72	0.97	44 ±45	0.99	75 ±39	0.98	76 ±26	0.99
Q1018+3056	-17 ±61	0.96	35 ±27	0.99	205 ±83	0.98	-44 ±83	0.98
Q1038+0625	-30 ±44	0.93	74 ±16	0.98	-112 ±10	0.97	-182 ±163	0.98
Q1120+0154	-67 ±94	0.92	-58 ±55	0.96	-644 ±82	0.97	···	···
Q1206+4557	51 ±82	0.93	36 ±129	0.93	-113 ±33	0.93	92 ±119	0.99
Q1241+1737	-3 ±51	0.93	···	0.98	348 ±281	0.81	-267 ±93	0.93
Q1247+0443	2 ±88	0.86	···	···	8 ±15	0.96	-29 ±29	0.98
Q1317+2743	223 ±96	0.84	···	···	159 ±26	0.98	264 ±37	0.96
Q1338+4138	123 ±61	0.91	122 ±51	0.93	-214 ±25	0.97	142 ±42	0.98
Q1340+2859	-84 ±147	0.87	···	···	180 ±18	0.94	-28 ±58	0.98
Q1356+5806	31 ±49	0.98	71 ±46	0.99	-248 ±14	0.99	···	···
Q1407+2632	270 ±43	0.81	···	···	-836 ±24	0.57	34 ±20	0.98
Q1458+7152	49 ±61	0.96	···	···	17 ±19	0.99	38 ±36	0.99
Q1522+1009	11 ±280	0.67	-10 ±105	0.94	62 ±26	0.94	···	···
Q1538+4745	-249 ±183	0.87	···	···	-650 ±83	0.89	40 ±101	0.96
Q1634+7037	58 ±64	0.97	21 ±52	0.97	-2 ±24	1.00	···	···
Q1637+5726	-20 ±57	0.88	···	···	67 ±36	0.84	-134 ±40	0.98
Q1656+0519	32 ±53	0.81	···	···	58 ±19	0.84	-4 ±34	0.96
Q1718+4807	24 ±92	0.86	···	···	54 ±44	0.93	34 ±83	0.93
Q1821+1042	35 ±56	0.94	54 ±19	0.99	-10 ±9	0.97	···	···
Q2145+0643	93 ±73	0.88	···	···	-19 ±47	0.97	···	···
Q2216−0350	200 ±67	0.82	···	···	-29 ±29	0.93	173 ±117	0.95

[a]The quoted errors are the formal errors from the cross-correlation analysis. As explained in § 3.2, we believe the true error is 100 km s^{-1}.

[b]"CCF" stands for the height of the cross-correlation peak.

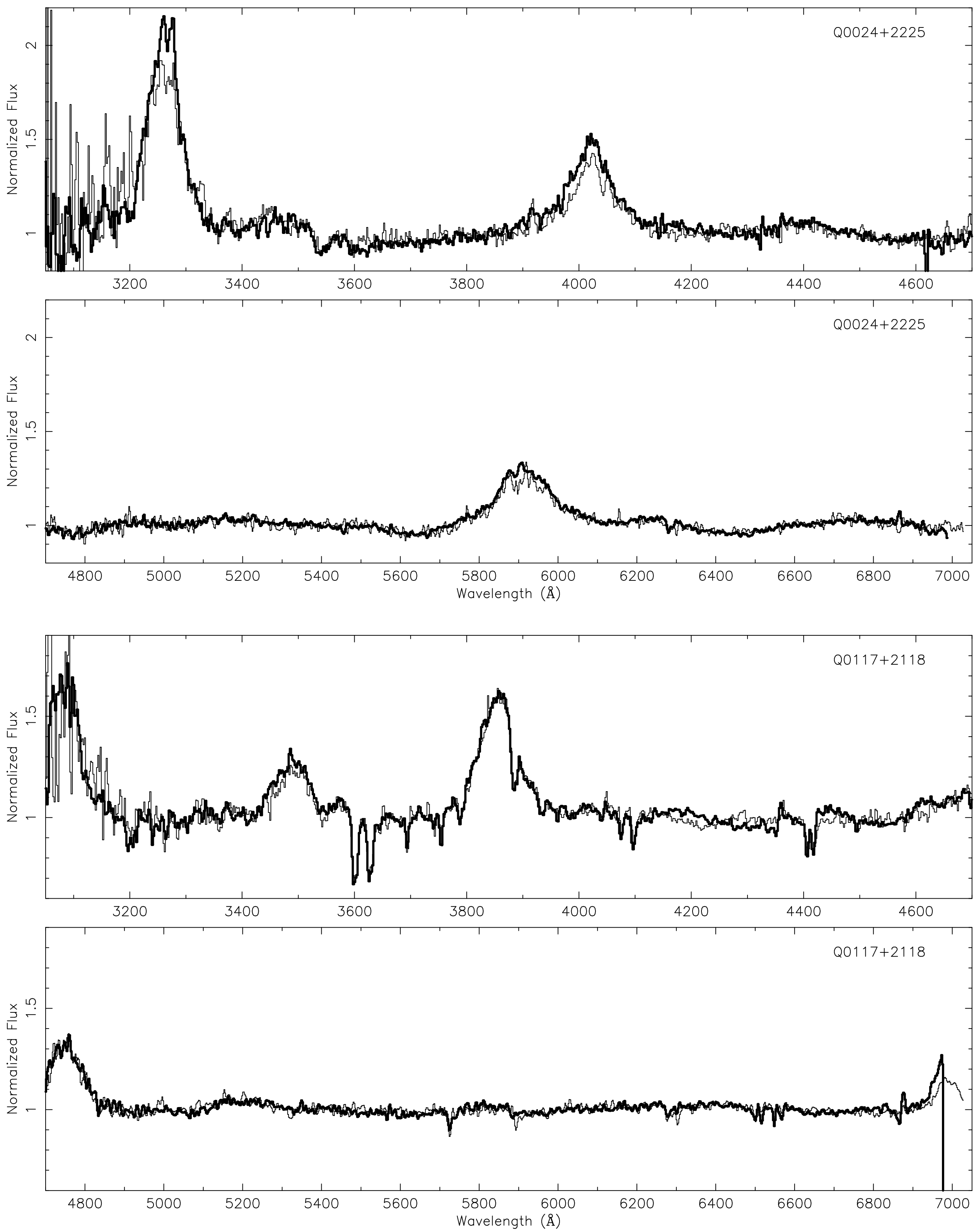

Fig. 1.— Continuum-flattened spectra of the 30 quasars in our survey. The blue and red spectra are displayed in separate panels for each object. The first epoch data are drawn with the heavier line.

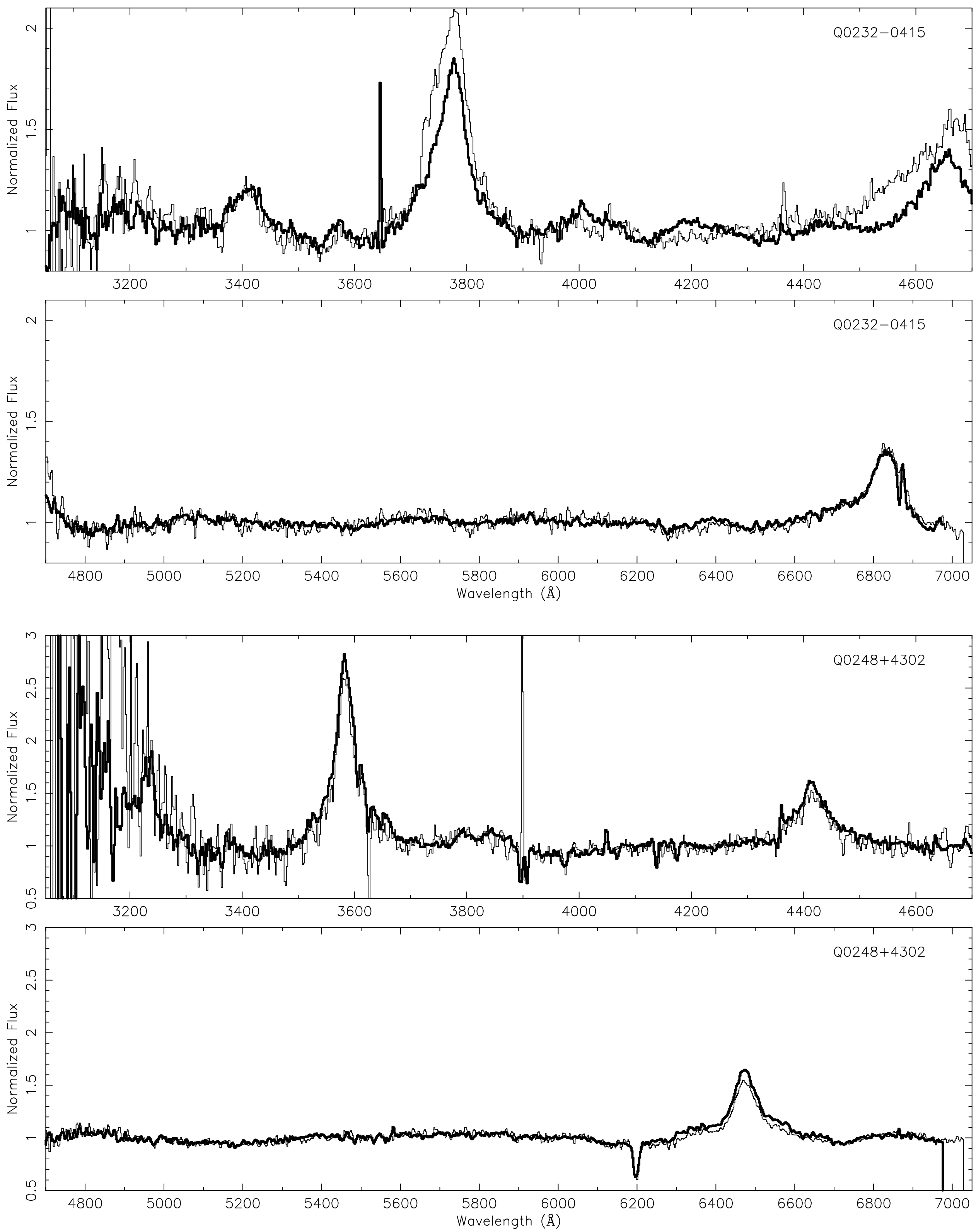

Fig. 1.— *Continued.*

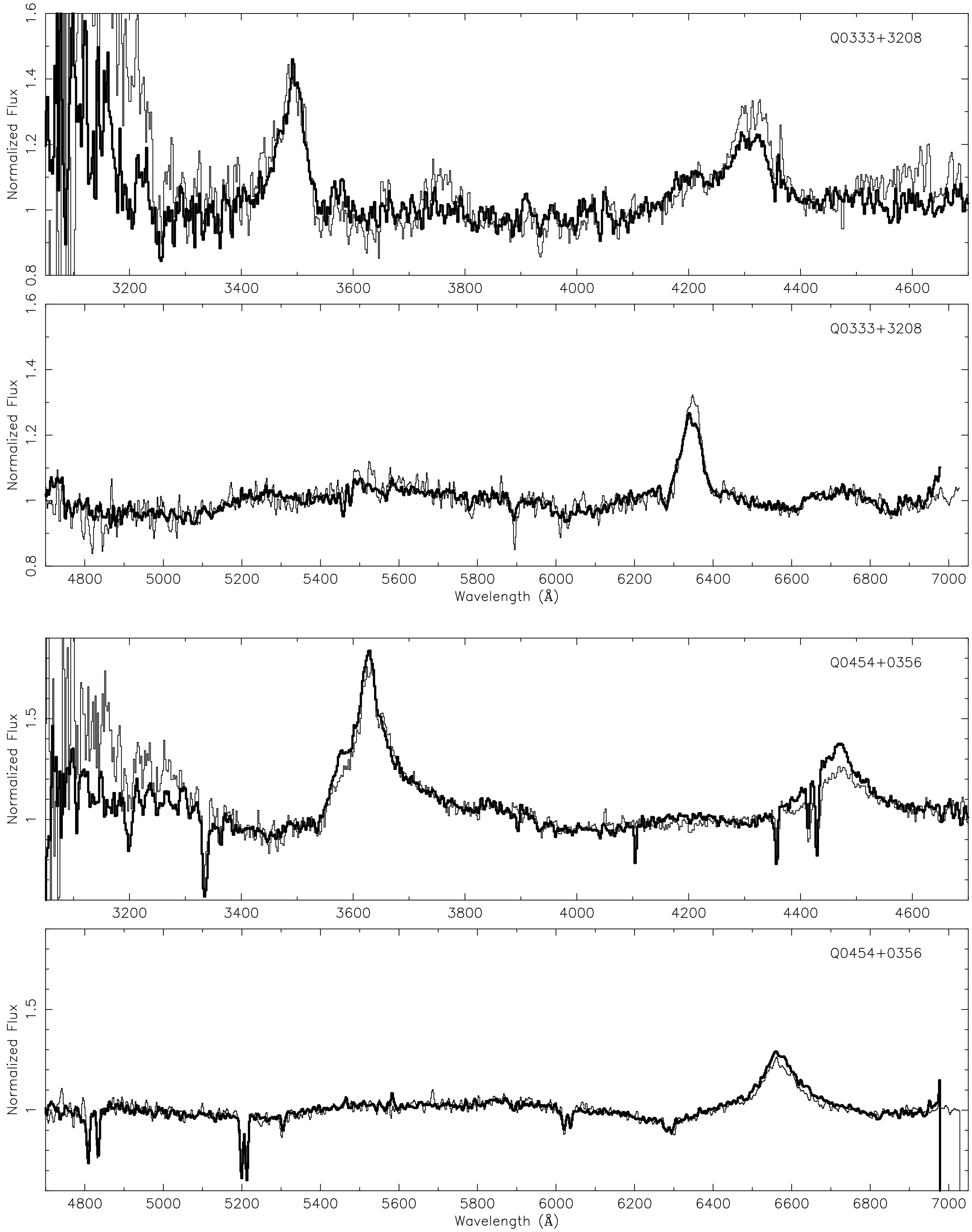

Fig. 1.— *Continued.*

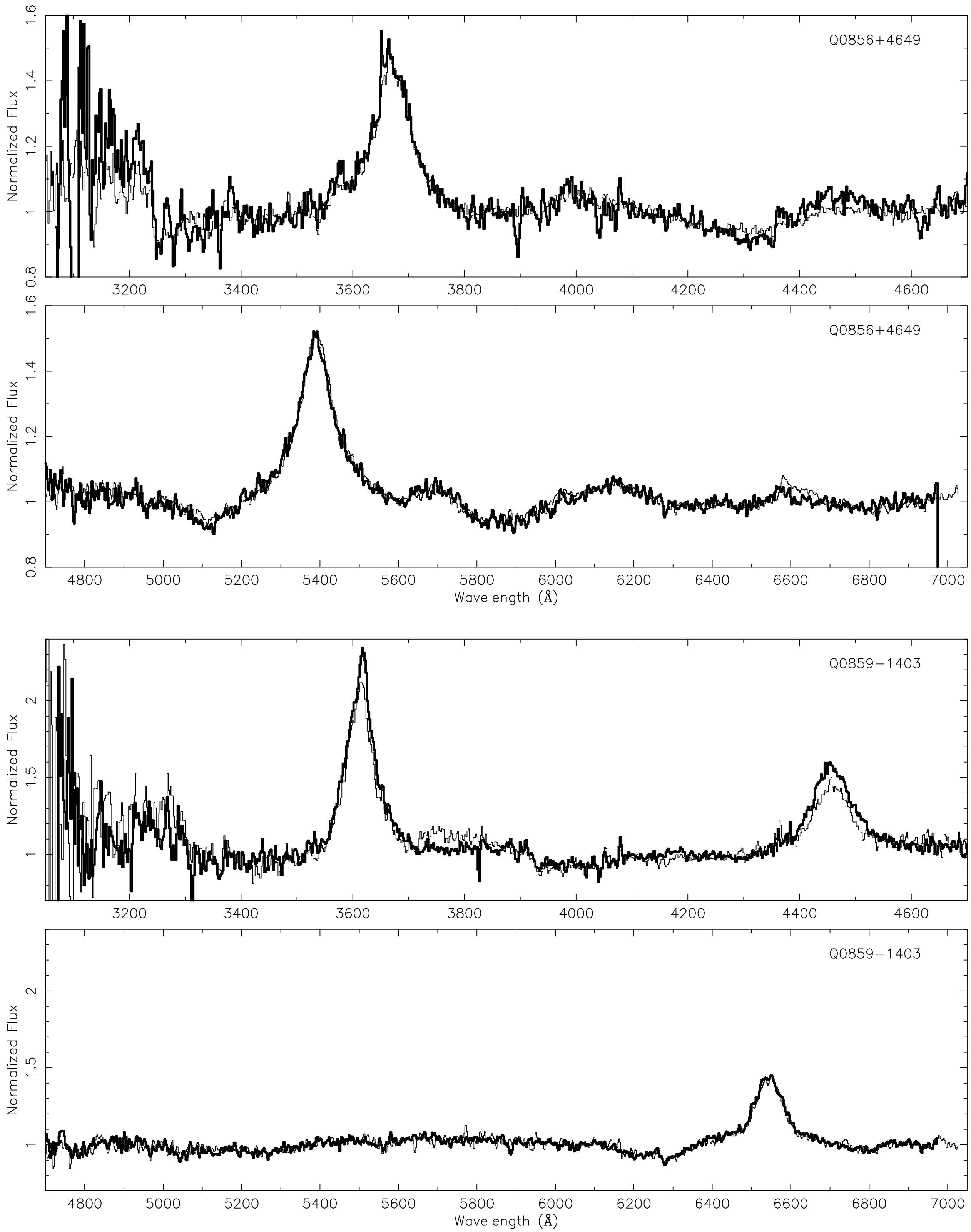

Fig. 1.— *Continued.*

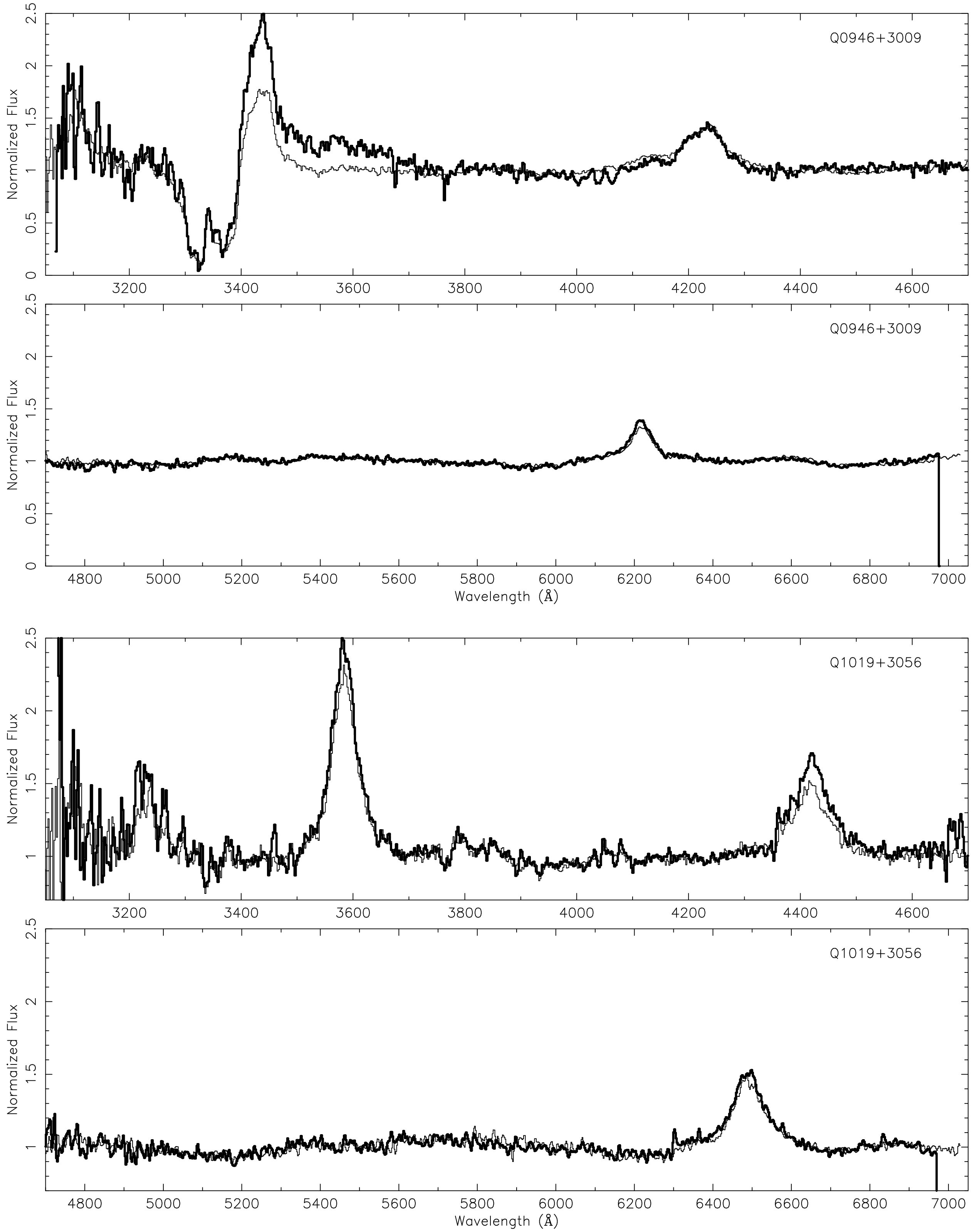

Fig. 1.— *Continued.*

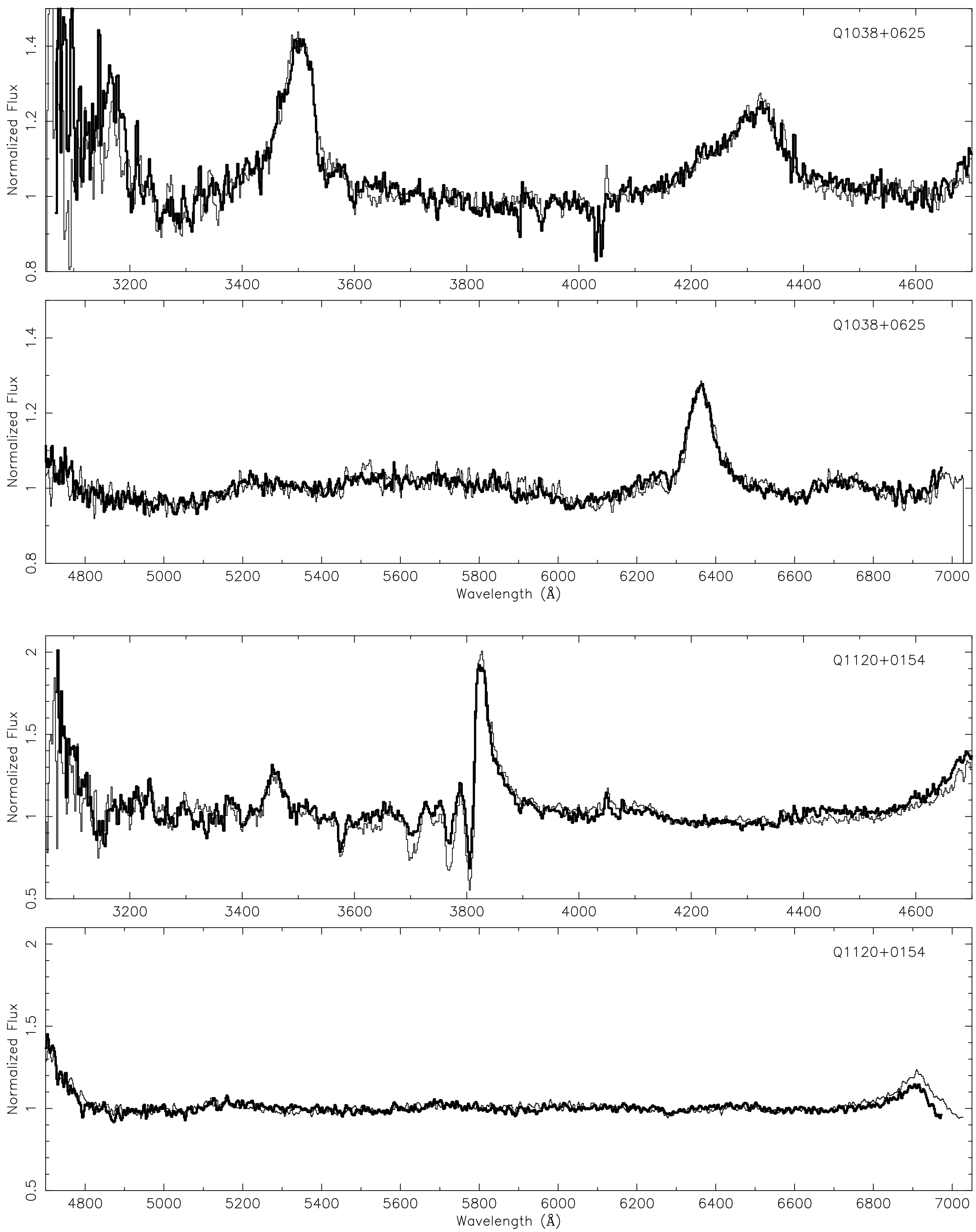

Fig. 1.— *Continued.*

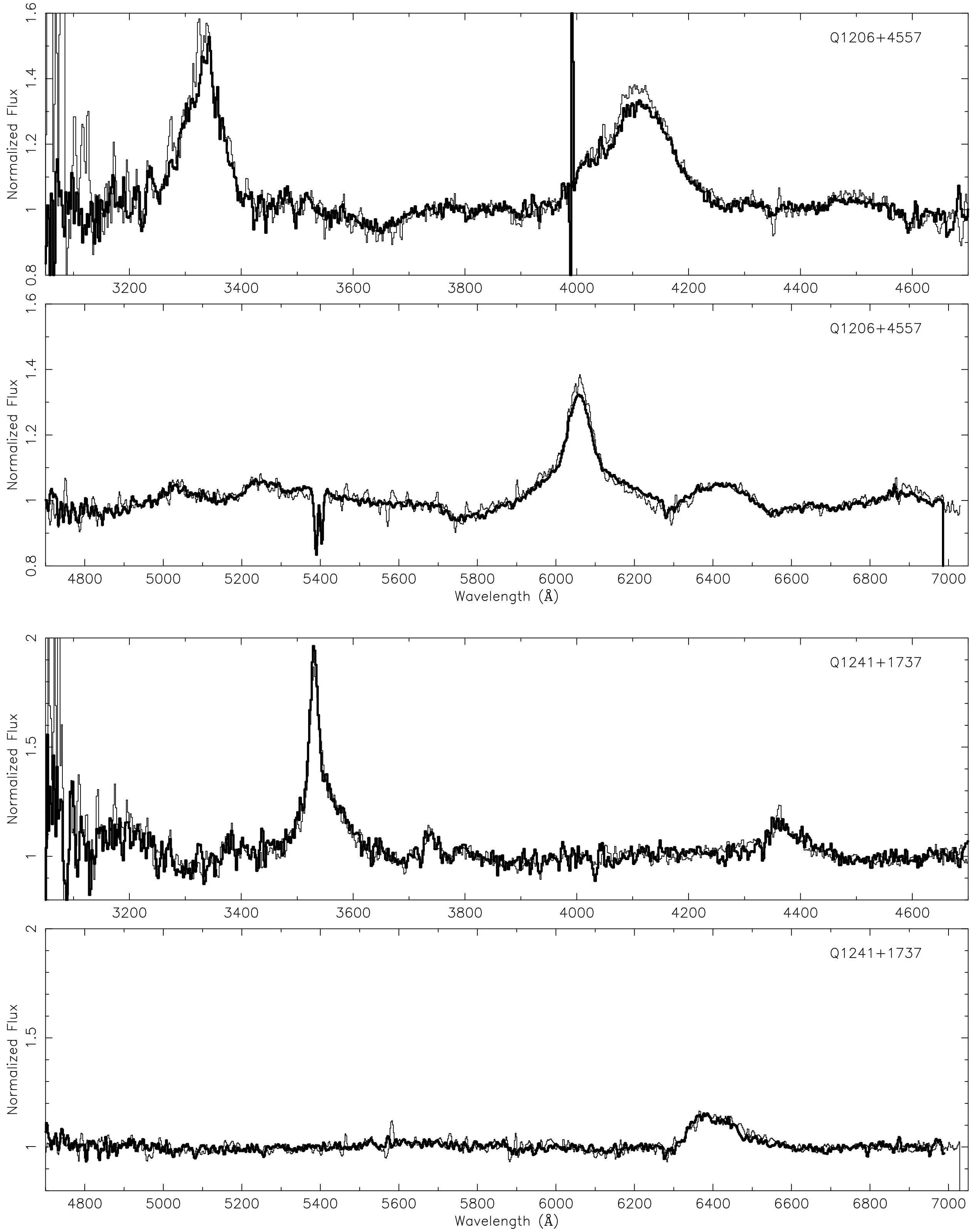

Fig. 1.— *Continued.*

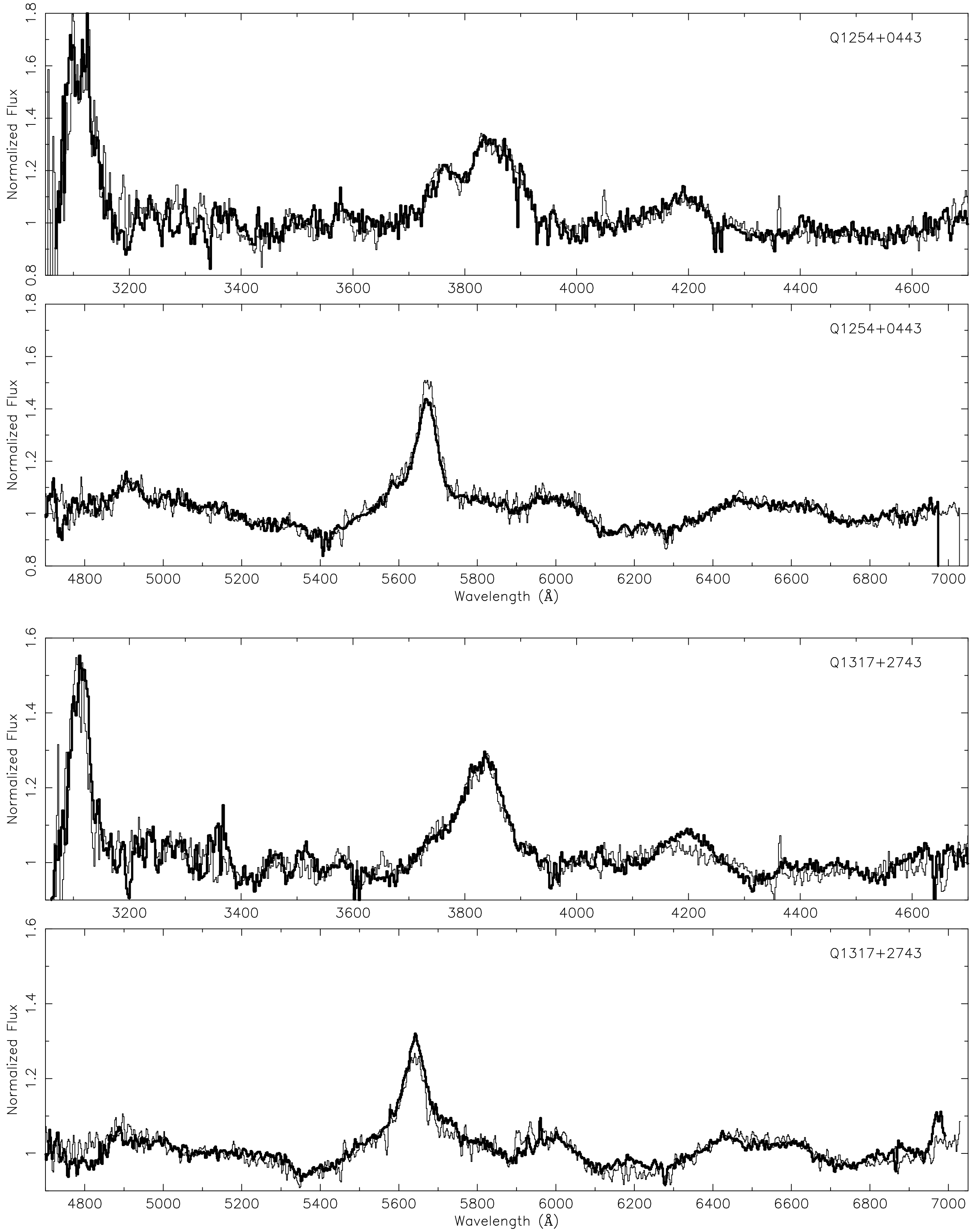

Fig. 1.— *Continued.*

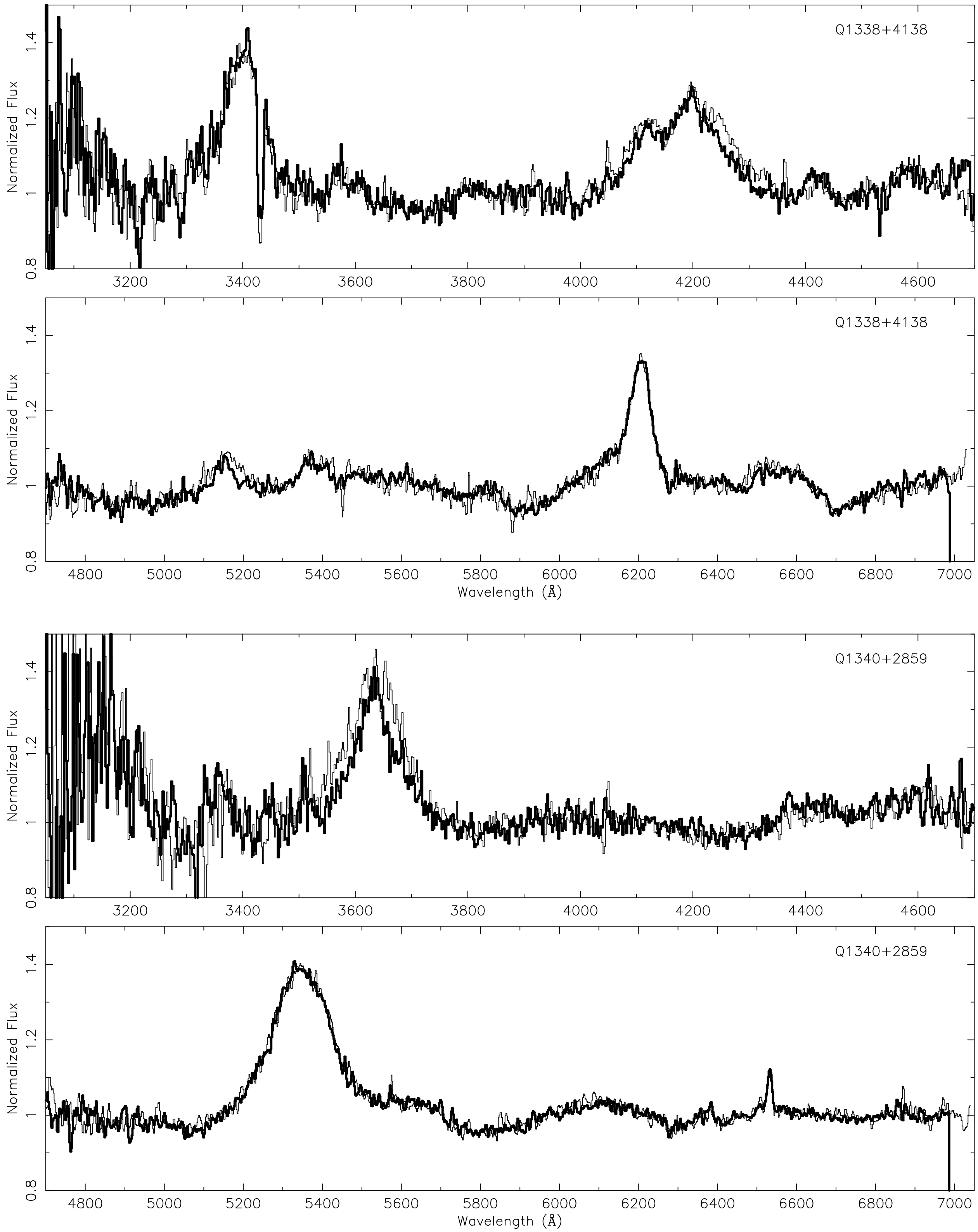

Fig. 1.— *Continued.*

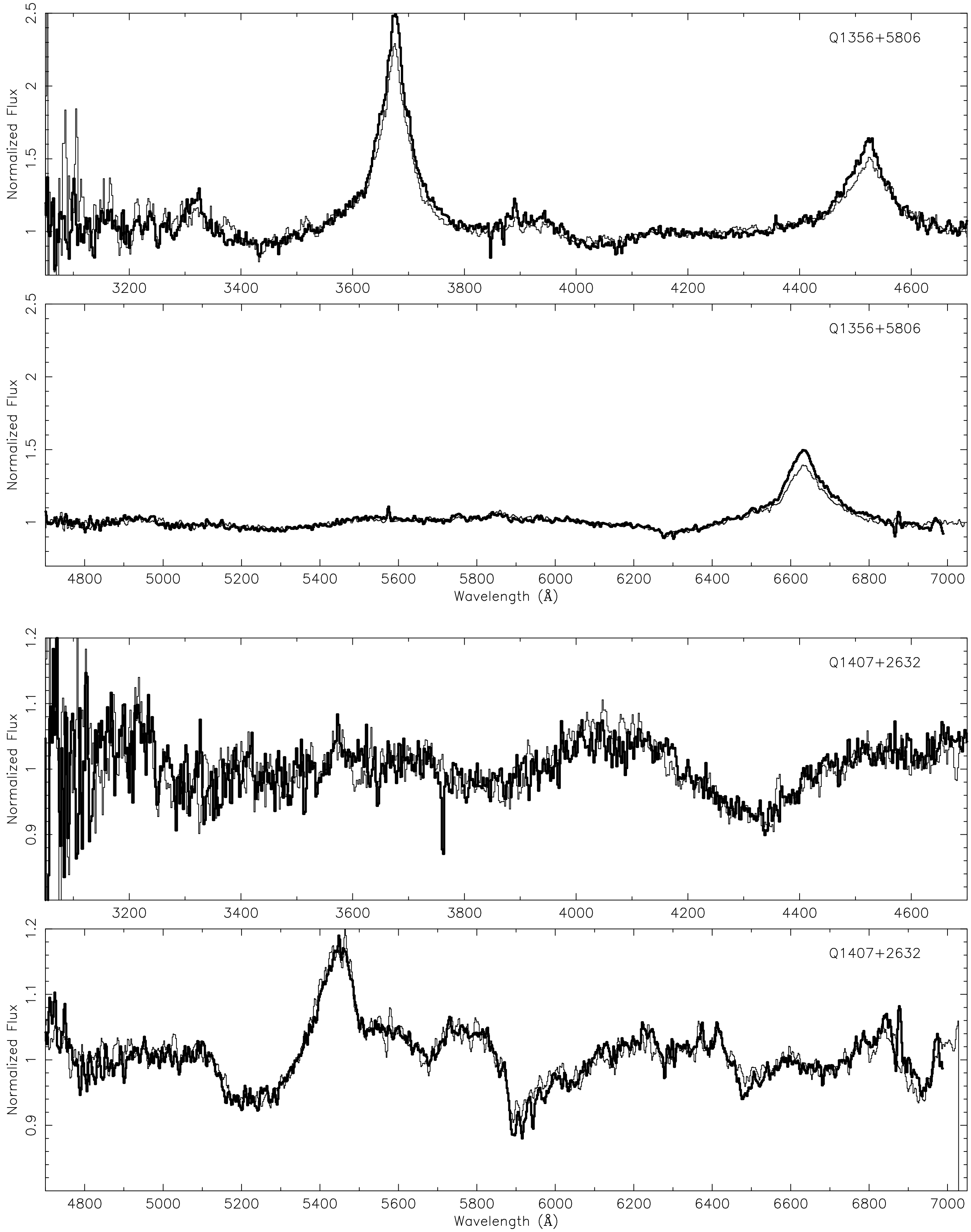

Fig. 1.— *Continued.*

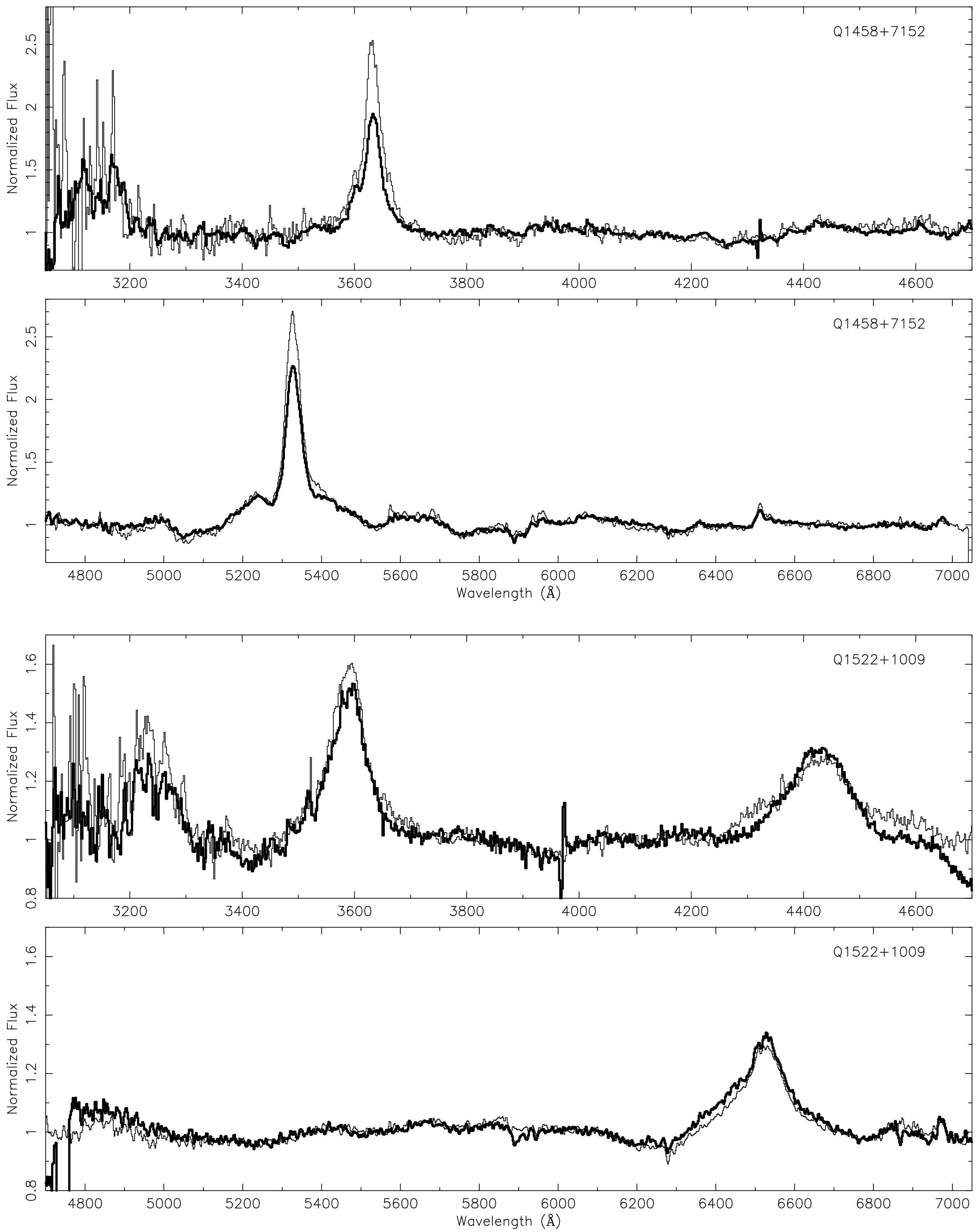

Fig. 1.— *Continued.*

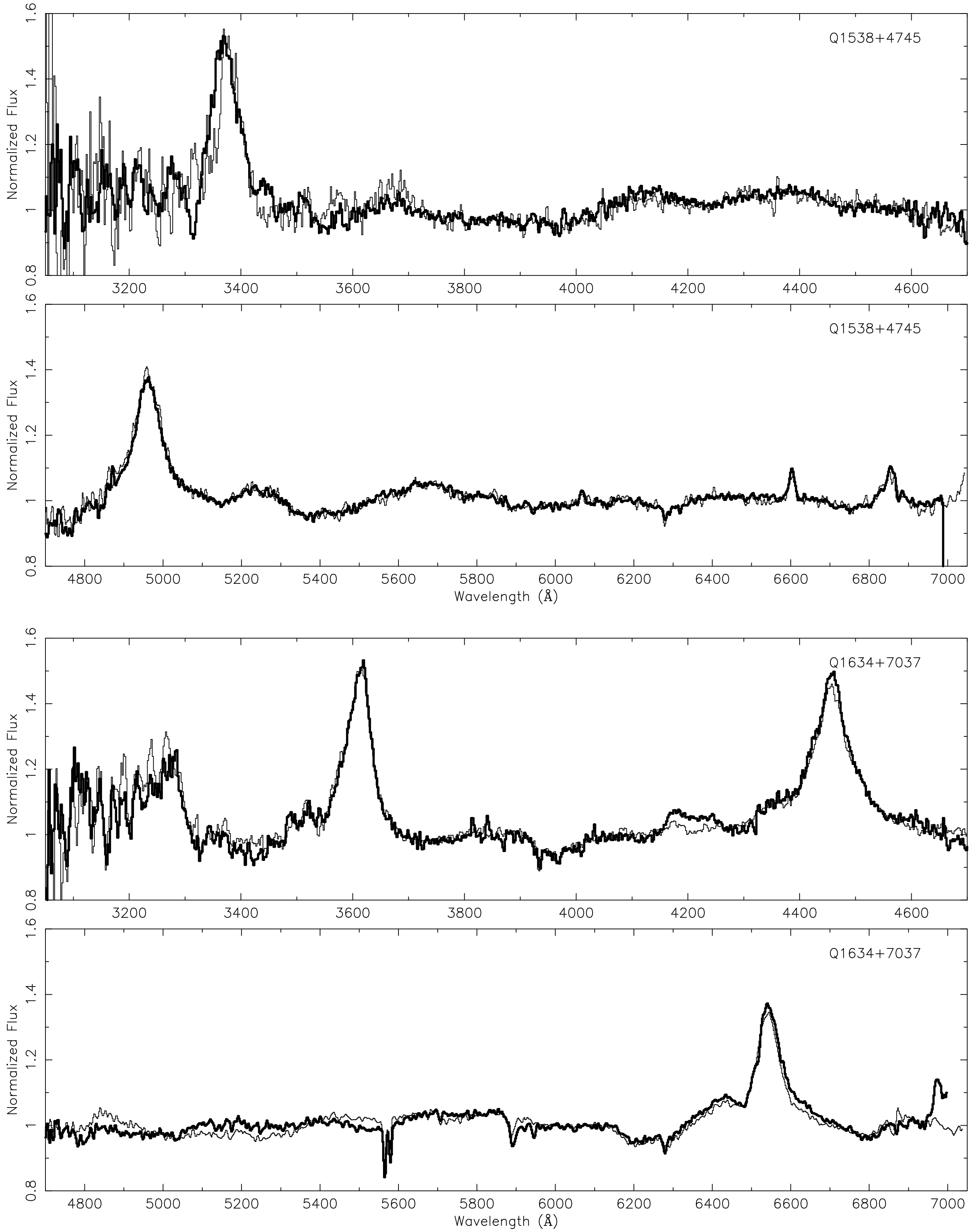

Fig. 1.— *Continued.*

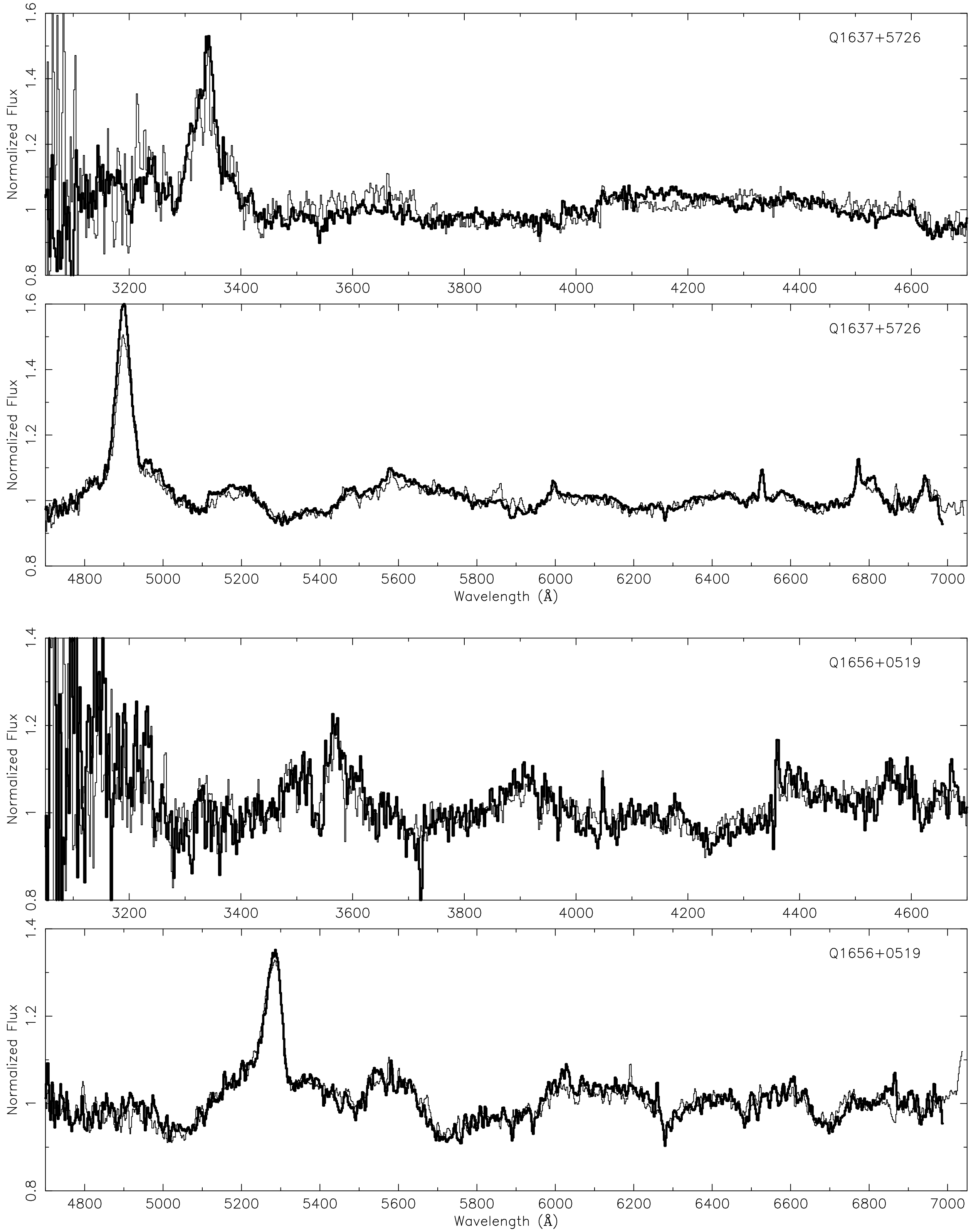

Fig. 1.— *Continued.*

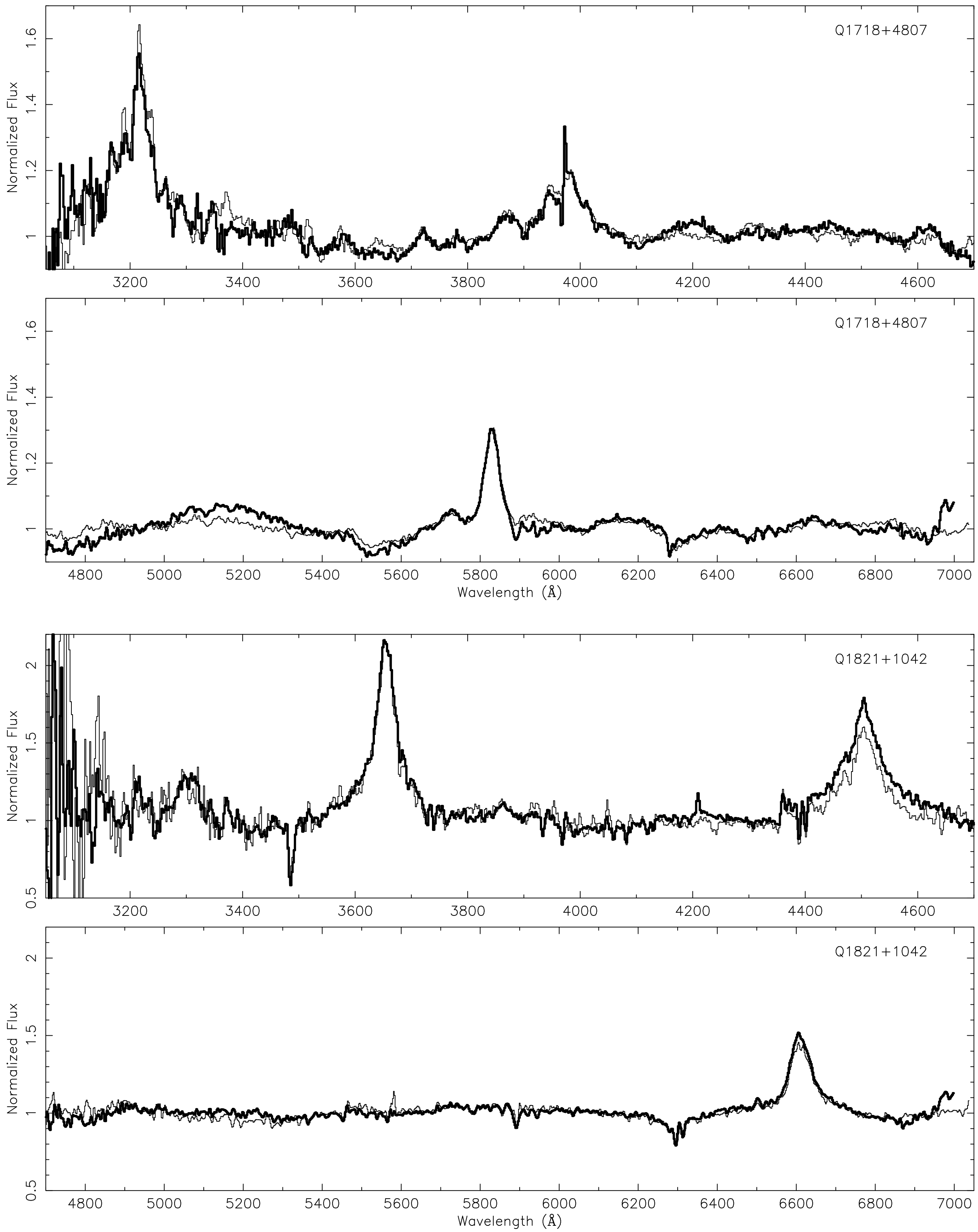

Fig. 1.— *Continued.*

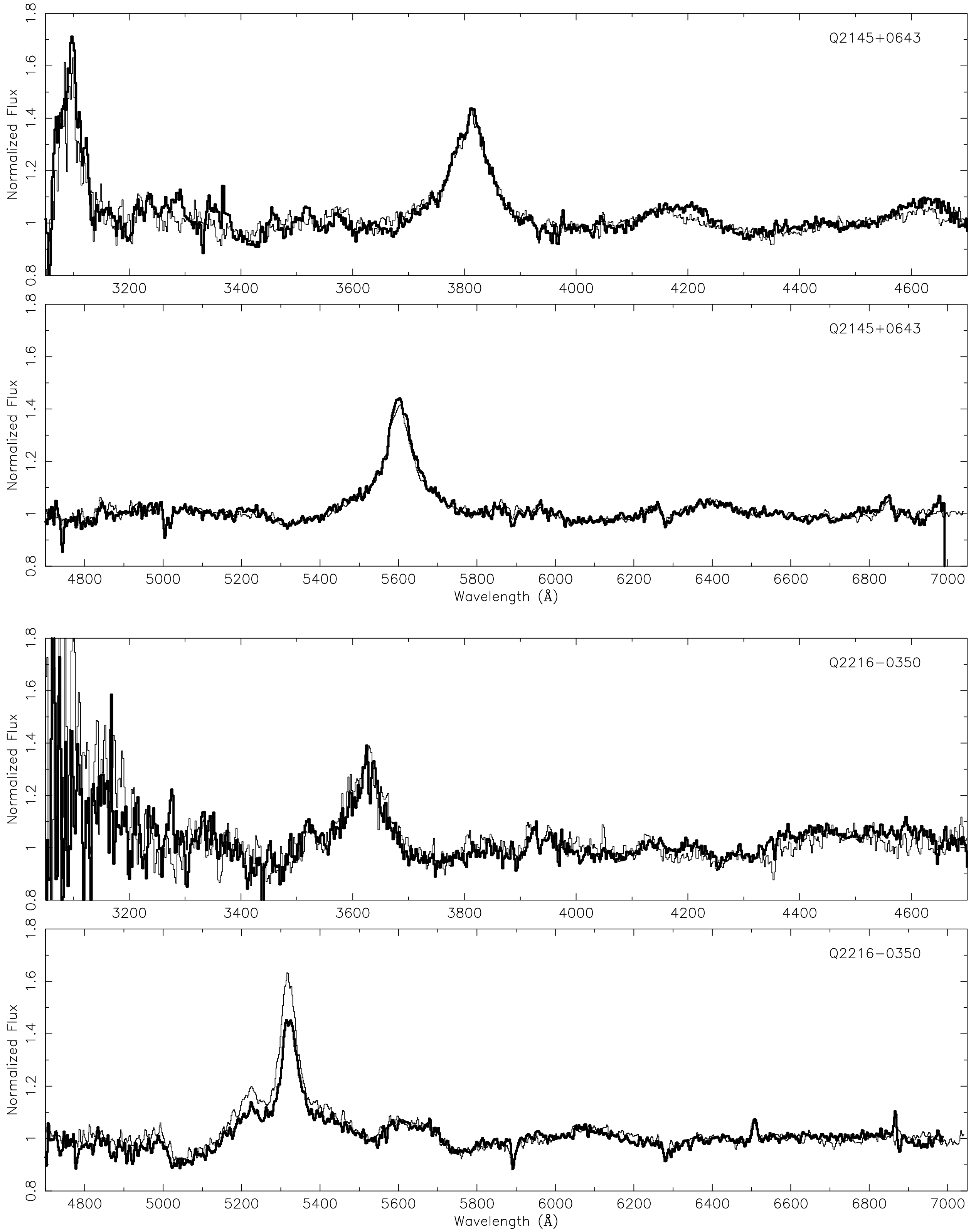

Fig. 1.— *Continued.*

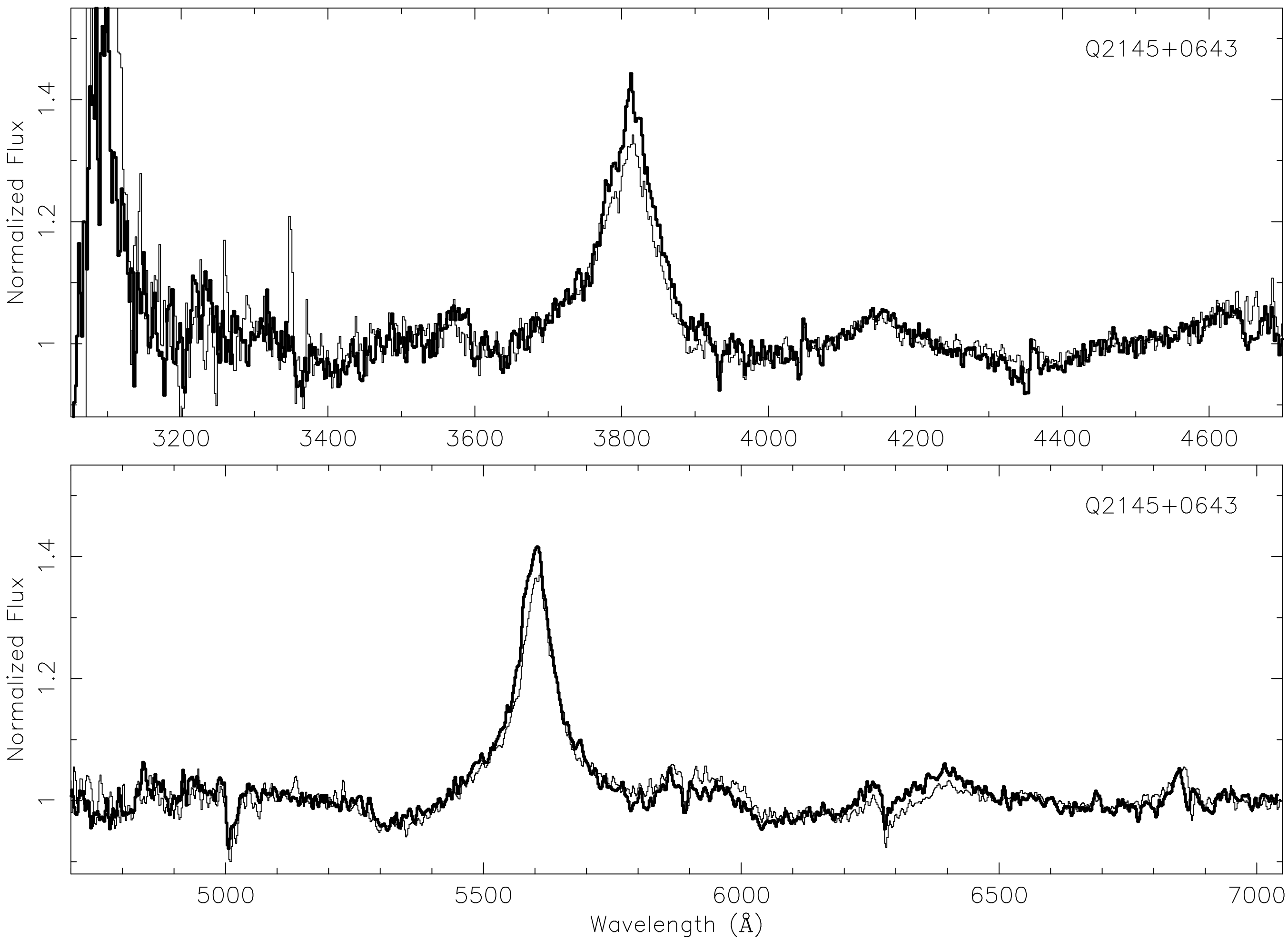

Fig. 2.— Continuum-flattened spectra of Q2145+0643. The blue and red spectra are displayed in separate panels. The second epoch spectrum is drawn with the heavier line. The spectrum from 1992 October 20 is drawn with the lighter line.

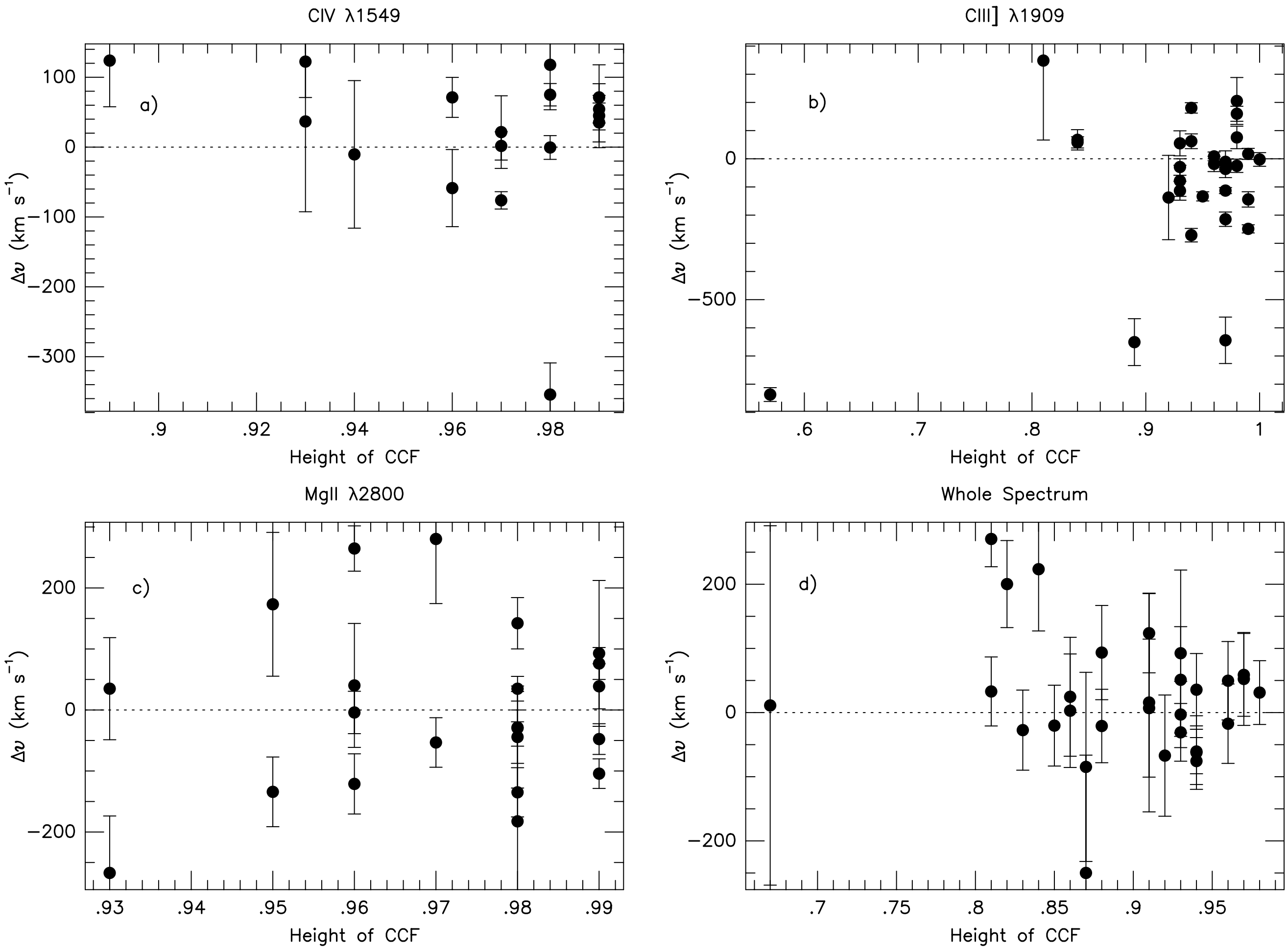

Fig. 3.— Results of the cross-correlation of spectra from the two epochs. The computed velocity difference is plotted against the cross-correlation peak height for the (a) C IV, (b) C III], and (c) Mg II emission lines and (d) for the whole observed wavelength range. The error bars show the formal errors from the cross-correlation analysis, although we take the true errors to be the rms velocity difference of the quasar pairs when whole wavelength range is correlated, 100 km s^{-1}. Note the different axis scales in each panel.